

## LETTERS

# Increase in African dust flux at the onset of commercial agriculture in the Sahel region

Stefan Mulitza<sup>1</sup>, David Heslop<sup>1</sup>, Daniela Pittauerova<sup>2</sup>, Helmut W. Fischer<sup>2</sup>, Inka Meyer<sup>1</sup>, Jan-Berend Stuut<sup>1,3</sup>, Matthias Zabel<sup>1</sup>, Gesine Mollenhauer<sup>1,4</sup>, James A. Collins<sup>1</sup>, Henning Kuhnert<sup>1</sup> & Michael Schulz<sup>1</sup>

The Sahara Desert is the largest source of mineral dust in the world<sup>1</sup>. Emissions of African dust increased sharply in the early 1970s (ref. 2), a change that has been attributed mainly to drought in the Sahara/Sahel region<sup>2</sup> caused by changes in the global distribution of sea surface temperature<sup>3,4</sup>. The human contribution to land degradation and dust mobilization in this region remains poorly understood<sup>5–11</sup>, owing to the paucity of data that would allow the identification of long-term trends in desertification<sup>12</sup>. Direct measurements of airborne African dust concentrations only became available in the mid-1960s from a station on Barbados<sup>2</sup> and subsequently from satellite imagery since the late 1970s: they do not cover the onset of commercial agriculture in the Sahel region ~170 years ago<sup>11,13,14</sup>. Here we construct a 3,200-year record of dust deposition off northwest Africa by investigating the chemistry and grain-size distribution of terrigenous sediments deposited at a marine site located directly under the West African dust plume. With the help of our dust record and a proxy record for West African precipitation<sup>15</sup> we find that, on the century scale, dust deposition is related to precipitation in tropical West Africa until the seventeenth century. At the beginning of the nineteenth century, a sharp increase in dust deposition parallels the advent of commercial agriculture in the Sahel region. Our findings suggest that human-induced dust emissions from the Sahel region have contributed to the atmospheric dust load for about 200 years.

We have constructed a long-term record of African dust deposition extending far beyond the instrumental record by investigating the chemistry and grain-size distribution of terrigenous sediments deposited at marine site GeoB9501 (16° 50' N, 16° 44' W), located on a shallow terrace on the northern flank of the Mauritania canyon at a water depth of 323 m. Today this location receives terrigenous sediments in the form of atmospheric dust and Senegal River suspension<sup>16</sup> (Fig. 1). The geochemical signatures of these two sources are very different (Supplementary Fig. 3). The Senegal River drains the western part of Guinea<sup>17</sup> and transports suspended matter derived from deeply weathered soils formed under tropical conditions far south of the modern river mouth. These lateritic soils, and hence the Senegal River suspension, are rich in aluminium and iron<sup>18</sup>. Approximately 95% of the particles delivered by the Senegal River are smaller than 10 µm (ref. 18). In contrast, coarse dust with particle sizes up to 200 µm (ref. 19) that is relatively rich in silicon<sup>20</sup> is mobilized in the Sahel and the western Sahara<sup>5</sup> from where it is transported to site GeoB9501 primarily by trade winds and within the Saharan Air Layer<sup>21</sup>. Instrumental data indicate that dust input and fluvial runoff are inversely related (Fig. 2b). Any change in continental precipitation should alter the relative proportions of atmospheric dust and

river suspension deposited on the continental margin off Senegal and Mauritania and hence should modify the grain-size distribution and geochemistry of the bulk sediments.

The record of site GeoB9501 has been derived from a 0.43-m-long multicore, documenting the most recent phase of sedimentation and a 5.32-m-long gravity core spanning the past 3,200 years (Fig. 2a). The age model for both cores is based on a combination of radiocarbon dating of planktonic foraminifera and <sup>210</sup>Pb/<sup>137</sup>Cs dating (Supplementary Methods and Supplementary Fig. 1). To quantify the relative proportions of atmospheric dust and Senegal suspension, we measured the downcore bulk concentration of Al, Si, Ca, K and Ti (Supplementary Methods). Representative dust and fluvial end-member compositions were constructed by bootstrapping the elemental concentration data of nine modern aeolian samples from the Sahara–Sahel Dust Corridor<sup>20</sup> and ten samples of suspended material from the Senegal River<sup>18</sup>. The relative abundances of the dust and fluvial end-members, along with a theoretical marine end-member (Supplementary Methods), were then determined by constrained non-negative least-squares applied throughout the sediment core.

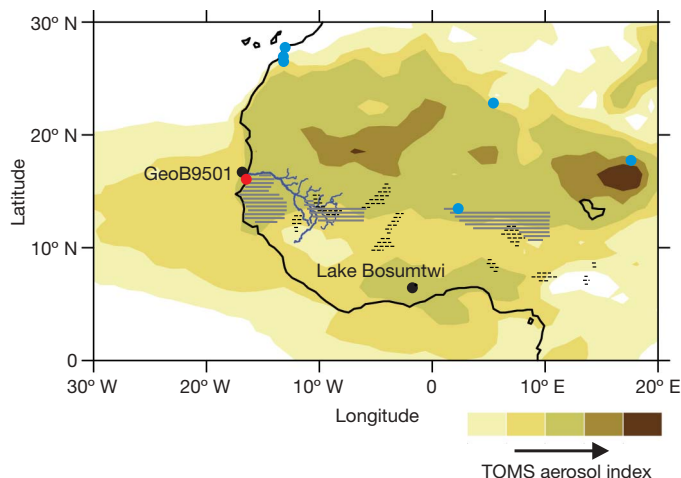


**Figure 1** | Locations of site GeoB9501 and Lake Bosumtwi. The Senegal River and tributaries are shown in blue and the averaged Total Ozone Mapping Spectrometer (TOMS) aerosol index for the years 1997–2005, highlighting the Sahara–Sahel Dust Corridor, is shaded in yellow to brown. (TOMS data are available at <http://toms.gsfc.nasa.gov/>.) Black dots show the locations of site GeoB9501 and Lake Bosumtwi. Also shown are the locations of dust/soil samples<sup>20</sup> (blue dots) and fluvial suspension samples<sup>18</sup> (red dot) used to construct the end-member model. Horizontal hatching indicates areas of commercial groundnut (solid) and cotton (dashed) production in 1914 AD (ref. 14).

<sup>1</sup>MARUM—Center for Marine Environmental Sciences, University of Bremen, Leobener Strasse, D-28359 Bremen, Germany. <sup>2</sup>Institute of Environmental Physics, University of Bremen, Otto-Hahn-Allee 1, D-28359 Bremen, Germany. <sup>3</sup>Royal Netherlands Institute for Sea Research, PO Box 59, 1790 AB Den Burg (Texel), The Netherlands. <sup>4</sup>Alfred Wegener Institute for Polar and Marine Research, 27515 Bremerhaven, Germany.

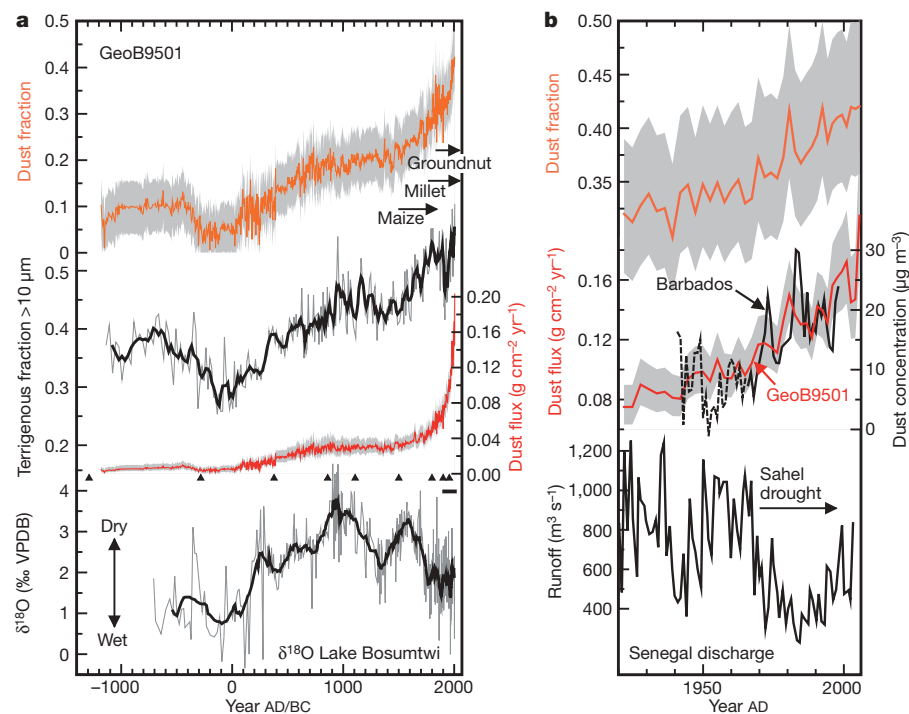


**Figure 2 | Comparison of dust deposition and precipitation records for the late Holocene.** **a**, The mean dust fraction (orange line) with grey shading showing the derived uncertainty envelope described in the Supplementary Methods, terrigenous grain-size fraction >10 μm (black line, smoothed with a five-point moving average), and dust deposition flux (red line with shaded 95% confidence interval) are shown for site GeoB9501 (top three traces). The δ<sup>18</sup>O of authigenic carbonates from Lake Bosumtwi<sup>15</sup> is shown as the bottom trace (grey raw data smoothed with a black 13-point moving average). VPDB, Vienna Pee-Dee Belemnite reference. Triangles indicate radiometric age-control points (Supplementary Table 1). The short horizontal black bar indicates the range of <sup>210</sup>Pb/<sup>137</sup>Cs dating. Horizontal arrows indicate the times at which maize, millet and groundnut agriculture became dominant. **b**, Shown are the mean dust fraction (orange line) with grey shading showing the derived uncertainty envelope, dust deposition flux (red line with shaded 95% confidence interval) at site GeoB9501 and instrumental records of atmospheric dust concentrations at Barbados<sup>2</sup> (black line) and the Senegal runoff (black bottom trace; redrawn from ref. 27). The horizontal arrow indicates the onset of Sahel drought in 1968. Barbados dust concentrations before 1966 (dashed black line) have been estimated<sup>2</sup> from regression with Sahel precipitation.

To determine mass accumulation rates, the relative contributions of the three end-members were multiplied by the product of dry bulk density and sedimentation rate (Supplementary Methods).

The <sup>210</sup>Pb/<sup>137</sup>Cs dated part of our record overlaps with the instrumental record and shows clearly that the increase of African dust emission observed from Barbados after 1968 (ref. 2) was associated with an increase in dust deposition flux at site GeoB9501 (Fig. 2b). The distribution and deposition of African dust is variable in space and time<sup>1</sup>. Moreover, Barbados receives most of its dust during the summer<sup>2</sup>, whereas the dust deposition flux at the African coast is highest during the winter months<sup>22</sup>. This seasonal and spatial heterogeneity is a plausible explanation for slight differences between the Barbados dust concentration and the dust deposition flux at site GeoB9501.

The evolution of the bulk geochemical and grain-size signature at site GeoB9501 indeed indicates pronounced changes in the source of terrigenous sediments over the past ~3,200 years (Fig. 2a). The oldest part of the record from about 1200 BC to about 200 AD is dominated (>78%) by fine-grained fluvial sediments. The next 700 years are characterized by a gradual increase in dust deposition and grain size, stabilizing around 900 AD. From the fourteenth century onwards, dust deposition rises again with the steepest increase of the entire record occurring after the early nineteenth century (Supplementary Fig. 4). Sedimentation rates increase along with the amount of dust deposition (Supplementary Fig. 2). Components of marine origin constitute only a minor proportion of the sediment (Supplementary Fig. 2), so the total sediment accumulation must therefore be primarily controlled by the lithogenic flux and not by marine production (Supplementary Notes).

Evidence that much of the natural variability in dust supply to site GeoB9501 is driven by continental precipitation comes from the oxygen isotope record of Lake Bosumtwi in Ghana<sup>15</sup>. The δ<sup>18</sup>O record from this lake is representative for precipitation in the Sahel<sup>15</sup> and close to the tropical source region of the Senegal River (Fig. 1). During the period from 100 AD to 900 AD a clear drying trend is visible in Lake Bosumtwi along with an increase in dust deposition at site GeoB9501. During the next 400 years precipitation on land increases and dust input stabilizes. Dust deposition increases again with

the onset of another long-lasting drought between 1400 and 1700 AD. The correlation between dust-deposition flux and Bosumtwi δ<sup>18</sup>O is statistically significant for the period from 700 BC to 1700 AD (taking into account long-term trends and serial dependence, Pearson's  $r = 0.4$  within a 95% confidence interval [0.19; 0.6]; see Supplementary Notes). Our calculation of robust Mahalanobis distances, based on the dust, fluvial and marine mass accumulation rates separated into century bins, indicates that the uppermost two time intervals (1800–1900 AD and 1900–2000 AD) are outlying with respect to the robust covariance structure of the GeoB9501 fluxes (see Supplementary Notes). In addition, from the eighteenth century onwards, the observed relation between continental precipitation and dust deposition breaks down as the two processes appear to become, at least partially, decoupled (Fig. 3).

Modern dust generation in the Sahel has been related to continental precipitation<sup>2</sup> and human activity<sup>7</sup>. The degree of human-induced dust mobilization in the Sahel is, however, controversial. Our data support the dominant role of continental precipitation for the period from 600 BC to 1700 AD. The increase in dust accumulation after about 1700 AD cannot be interpreted exclusively by a decrease in precipitation over West Africa. After about 1700 AD precipitation increases to intermediate levels again, whereas the dust deposition continues to increase towards the present, at rates unprecedented during the preceding three millennia. Although the drought in the 1970s and 1980s was devastating and substantially contributed to increased atmospheric dust concentrations in the last decades<sup>2</sup>, it did not reach the magnitude of past multicentury-long droughts<sup>15</sup>, which resulted in the water level of Lake Bosumtwi dropping by more than 30 m.

The departure of the dust deposition from its long-term relation to precipitation coincides with a marked change in the agricultural regime in the western Sahel. Maize, introduced by the Portuguese, was a dominant crop of the early eighteenth century and was gradually replaced by the low-yielding millet and sorghum in the mid-eighteenth century (ref. 11) (Fig. 2a). The steepest increase in dust deposition, however, parallels the advent of commercial agriculture in Senegal, Nigeria and Gambia in the mid-nineteenth century, the so-called “cash crop revolution”<sup>11,14</sup>. Groundnuts were introduced to Senegal in 1840 and caused a rapid expansion of agricultural lands, encroachment on

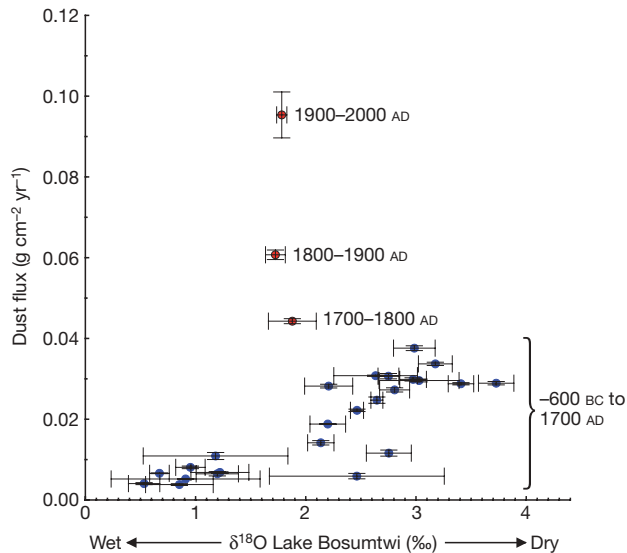


**Figure 3 | Relationship between  $\delta^{18}\text{O}$  of authigenic carbonates from Lake Bosumtwi<sup>15</sup> and dust deposition flux at site GeoB9501.** Low  $\delta^{18}\text{O}$  values denote wet conditions over West Africa. The positions of the 100-year-interval bins refer to their median values, while the displayed error bars represent the standard errors on the medians. For the unbinned data a significant linear correlation exists between dust flux and  $\delta^{18}\text{O}$  between 700 BC and 1700 AD (blue dots represent this time interval in the binned data; see Supplementary Notes). Based on the calculation of robust Mahalanobis distances from the GeoB9501 flux data, the bins spanning 1800–1900 AD and 1900–2000 AD do not follow the robust pattern of the dust, fluvial and marine mass accumulation rates and can be deemed to be outlying (Supplementary Notes). In terms of their relationship to conditions over West Africa, the two youngest bins are characterized by apparently high dust production for the given level of precipitation.

forests and woodlands and exposure of the soil to wind erosion<sup>13,23</sup>. In the early twentieth century, agricultural export economies were common in the West African Sahel<sup>14</sup>, a few hundred kilometres to the south of the modern centres of dust production (Fig. 1) and consistent with a southward shift of the economic centres of export production<sup>11</sup>.

It is plausible that the increased human-induced dust production also contributed to locally drier conditions in the Sahel by reducing the monsoonal rainfall via a direct cooling of the surface<sup>24,25</sup>. This process could enhance the observed decoupling of the precipitation in tropical West Africa and Sahelian dust generation that has prevailed since the eighteenth century (Fig. 2a) and which would explain the continuous desertification trend in the Sahel over the past four centuries, reported in historical sources<sup>11</sup>.

Satellite data suggest no systematic trend in desertification<sup>26</sup> and human dust mobilization from 1980 to the present. Our data show that a considerable increase in African dust emissions occurred with the onset of agricultural irrigation of Sahelian soils about two centuries ago and therefore too early for instrumental detection.

Received 3 September 2009; accepted 24 May 2010.

1. Engelstaedter, S., Tegen, I. & Washington, R. North African dust emissions and transport. *Earth Sci. Rev.* **79**, 73–100 (2006).
2. Prospero, J. M. & Lamb, P. J. African droughts and dust transport to the Caribbean: climate change implications. *Science* **302**, 1024–1027 (2003).
3. Folland, C. K., Palmer, T. N. & Parker, D. E. Sahel rainfall and worldwide sea temperatures, 1901–85. *Nature* **320**, 602–607 (1986).
4. Giannini, A., Saravanan, R. & Chang, P. Oceanic forcing of Sahel rainfall on interannual to interdecadal time scales. *Science* **302**, 1027–1030 (2003).
5. Prospero, J. M., Ginoux, P., Torres, O., Nicholson, S. E. & Gill, T. E. Environmental characterization of global sources of atmospheric soil dust identified with the Nimbus 7 Total Ozone Mapping Spectrometer (TOMS) absorbing aerosol product. *Rev. Geophys.* **40**, 1002, doi: 10.1029/2000RG000095 (2002).

6. Hein, L. & de Ridder, N. Desertification in the Sahel: a reinterpretation. *Glob. Change Biol.* **12**, 751–758 (2006).
7. Mahowald, N. M. *et al.* Understanding the 30-year Barbados desert dust record. *J. Geophys. Res.* **107**, 4561, doi: 10.1029/2002JD002097 (2002).
8. Nicholson, S. E., Tucker, C. J. & Ba, M. B. Desertification, drought, and surface vegetation: an example from the West African Sahel. *Bull. Am. Meteorol. Soc.* **79**, 815–829 (1998).
9. Prince, S. D., Wessels, K. J., Tucker, C. J. & Nicholson, S. E. Desertification in the Sahel: a reinterpretation of a reinterpretation. *Glob. Change Biol.* **13**, 1308–1313 (2007).
10. Tegen, I. & Fung, I. Contribution to the atmospheric mineral aerosol load from land-surface modification. *J. Geophys. Res.* **100**, 18707–18726 (1995).
11. Webb, J. L. A. *Desert Frontier: Ecological and Economic Change Along the Western Sahel 1600–1850* (University of Wisconsin Press, 1995).
12. Brooks, N. *et al.* The climate-environment-society nexus in the Sahara from prehistoric times to the present day. *J. N. Afr. Stud.* **10**, 253–292 (2005).
13. Mbow, C., Mertz, O., Diouf, A., Rasmussen, K. & Reenberg, A. The history of environmental change and adaptation in eastern Saloum–Senegal—Driving forces and perceptions. *Glob. Planet. Change* **64**, 210–221 (2008).
14. Austin, G. Cash crops and freedom: export agriculture and the decline of slavery in colonial West Africa. *Int. Rev. Soc. Hist.* **54**, 1–37 (2009).
15. Shanahan, T. M. *et al.* Atlantic forcing of persistent drought in West Africa. *Science* **324**, 377–380 (2009).
16. Koopmann, B. Sedimentation von Sahara Staub im subtropischen Nordatlantik während der letzten 25.000 Jahre. *Met. Forsch. Erg. C* **35**, 23–59 (1981).
17. Kattan, Z., Gac, J. Y. & Probst, J. L. Suspended sediment load and mechanical erosion in the Senegal Basin—estimation of the surface runoff concentration and relative contributions of channel and slope erosion. *J. Hydrol.* **92**, 59–76 (1987).
18. Gac, J. Y. & Kane, A. Le fleuve Sénégal: I. Bilan hydrologique et flux continentaux de matières particulaires à l'embouchure. *Sci. Geol. Bull.* **39**, 99–130 (1986).
19. Stuut, J. B. *et al.* Provenance of present-day eolian dust collected off NW Africa. *J. Geophys. Res.* **110**, D04202, doi: 10.1029/2004JD005161 (2005).
20. Moreno, T. *et al.* Geochemical variations in aeolian mineral particles from the Sahara-Sahel Dust Corridor. *Chemosphere* **65**, 261–270 (2006).
21. Prospero, J. M. & Carlson, T. N. Saharan air outbreaks over the tropical North Atlantic. *Pure Appl. Geophys.* **119**, 677–691 (1981).
22. Orange, D. & Gac, J. Y. Bilan géochimique des apports atmosphériques en domaines sahélien et soudano-guinéen d'Afrique de l'Ouest (bassins supérieurs du Sénégal et de la Gambie). *Geodynamique* **5**, 51–55 (1990).
23. Sterk, G. Causes, consequences and control of wind erosion in Sahelian Africa: a review. *Land Degrad. Dev.* **14**, 95–108 (2003).
24. Solmon, F. *et al.* Dust aerosol impact on regional precipitation over western Africa, mechanisms and sensitivity to absorption properties. *Geophys. Res. Lett.* **35**, L24705, doi: 10.1029/2008GL035900 (2008).
25. Yoshioka, M. *et al.* Impact of desert dust radiative forcing on Sahel precipitation: relative importance of dust compared to sea surface temperature variations, vegetation changes, and greenhouse gas warming. *J. Clim.* **20**, 1445–1467 (2007).
26. Tucker, C. J., Dregne, H. E. & Newcomb, W. W. Expansion and contraction of the Sahara Desert from 1980 to 1990. *Science* **253**, 299–301 (1991).
27. Isupova, M. V. & Mikhailov, V. N. Hydrological and morphological processes in Senegal River mouth area. *Water Res.* **35**, 30–42 (2008).

Supplementary Information is linked to the online version of the paper at [www.nature.com/nature](http://www.nature.com/nature).

**Acknowledgements** Radiocarbon datings were performed at the Leibniz-Laboratory for Radiometric Dating and Stable Isotope Research in Kiel and at the Poznan Radiocarbon Laboratory. This work was funded through the DFG Research Center/Cluster of Excellence “The Ocean in the Earth System”. We thank M. Prange for plotting the TOMS data in Fig. 1 and U. Röhl, K. Enneking, V. Lukies and M. Klann for technical support.

**Author Contributions** S.M. designed the study, took the cores, measured XRF data and wrote the manuscript. D.H. calibrated the data, and calculated the end-member model. D.P. and H.W.F. performed <sup>210</sup>Pb and <sup>137</sup>Cs dating, aligned the multicore and the gravity core and provided part of the age model. J.-B.S. and I.M. performed grain-size analyses. M.Z. performed the EDP-XRF analyses for calibration. M.S. and D.H. performed the statistical analyses. G.M. calculated the reservoir age and provided the age model for the gravity core. All authors contributed to the interpretation of the data.

**Author Information** Data have been submitted to the Publishing Network for Geoscientific & Environmental Data (PANGAEA, [www.pangaea.de](http://www.pangaea.de)). Reprints and permissions information is available at [www.nature.com/reprints](http://www.nature.com/reprints). The authors declare no competing financial interests. Readers are welcome to comment on the online version of this article at [www.nature.com/nature](http://www.nature.com/nature). Correspondence and requests for materials should be addressed to S.M. ([smulitza@uni-bremen.de](mailto:smulitza@uni-bremen.de)).